Land Mine Detection Using a Ground-Penetrating Radar Based on Resistively Loaded Vee Dipoles

Thomas P. Montoya, *Member, IEEE*, and Glenn S. Smith, *Fellow, IEEE*

***Abstract*—Resistively loaded Vee dipoles are considered for use in a short-pulse ground penetrating radar (GPR) used to detect buried antipersonnel land mines. First, a study is made to select a short pulse to radiate that is most appropriate for the problem. A simple one-dimensional (1-D) analysis of some representative soils and a land mine is used to select a radiated pulse similar in shape to a differentiated Gaussian pulse with a spectral peak at 4 GHz. Based on previous studies, the conductivity of the arms of the Vee dipole is linearly tapered from the feed to the open ends. A fully three-dimensional (3-D) finite-difference time-domain (FDTD) model is developed and used to simulate the GPR land mine detection problem. Using this model, a resistively loaded Vee dipole is selected and evaluated. Parametric studies related to the problem are conducted including: varying the height of the Vee above the ground, varying the position of the land mine both laterally and in depth, and examining the effects of the geometry of the land mine on the received signal. Environmental conditions are examined including signal returns from rocks and variations in the shape of the surface of the ground. The FDTD results are validated by comparisons with experimental data. These studies demonstrate that resistively loaded Vee dipoles can greatly reduce clutter related to the antenna, making the task of distinguishing land mines (targets) much easier.**

***Index Terms*—Finite-difference time-domain (FDTD), ground-penetrating radar (GPR), land mines.**

I. Introduction

A short-pulse ground-penetrating radar (GPR) radiates a temporally short pulse into the ground to detect buried objects, e.g., land mines. A problem motivating research into GPR systems is the crisis of an estimated 80–110 million land mines spread throughout the world [1], [2]. Antipersonnel land mines are of particular concern as they injure thousands of civilians each year. Metal detectors and mechanical probing, currently the primary means of detecting and locating land mines, are inadequate and/or dangerous for finding land mines with low metal content (made of ceramics, explosives, and plastics). The small size of many antipersonnel land mines (largest dimension less than 10 cm) necessitates the use of a short pulse (duration less than 1 ns) with GPR systems.

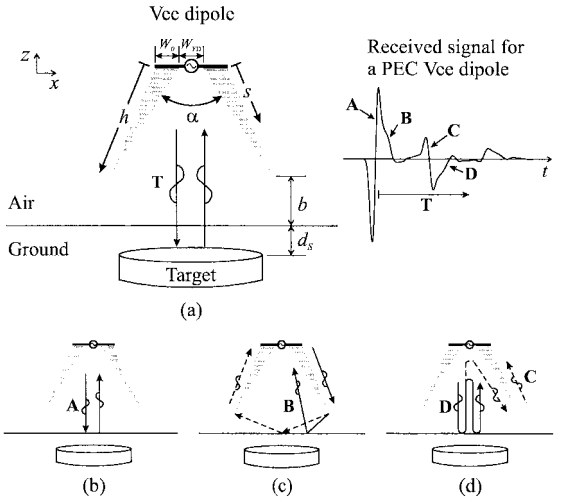

Fig. 1. Geometry for the problem showing (a) the reflection from the target; (b) and (c) the initial reflections from the surface of the ground; and (d) the multiple reflections between the surface of the ground and the antenna and the reflection internal to the antenna due to the initial reflection from the ground.

A broad-band directive antenna is required to transmit a short pulse into a spot on the ground. The spot illuminated on the ground should be no larger than the geometrical cross section of the target in order to maximize the ratio of the target signal to the background, e.g., signal due to the reflection from the surface of the ground, and to resolve the location of the target. Here, the resistively loaded Vee dipole is studied to demonstrate that it is suitable for a short-pulse GPR used for detecting buried antipersonnel land mines. Previous studies [3], [4] indicated that a resistively loaded Vee dipole where the conductivity is linearly tapered from the feed point to the open end has the best performance.

Fig. 1 shows the geometry of the problem where the antenna is located above the target buried in the ground. For a monostatic GPR, the antenna radiates a pulse and receives the pulses reflected from the buried target (**T**) and the surface of the ground (**A**). Ideally, the voltage reflected at the drive point (feed) and open ends of the antenna should be small, the radiated signal should be as large as possible, and clutter should be minimized so as not to obscure the return from the target. Sources of clutter include radiation from the open ends

Manuscript received September 25, 1998; revised October 4, 1999. This work was supported in part by the Joint Services Electronics Program (JSEP) under Contract DAAH04-96-1-0161, the Army Research Office under Contracts DAAH-04-94-G-0144 and DAAG55-98-1-0403, and the Advanced Research Projects Agency (ARPA) through a National Defense Science and Engineering Graduate (NDSEG) Fellowship.

T. P. Montoya is with the Department of Electrical Engineering, University of Tennessee, Knoxville, TN 37996-2100 USA.

G. S. Smith is with the School of Electrical and Computer Engineering, Georgia Institute of Technology, Atlanta, GA 30332-0250 USA.

Publisher Item Identifier S 0018-926X(99)09981-0.

of the antenna that is reflected by the ground (**B**), reflections internal to the antenna that are generated when a signal is received (**C**), and multiple reflections between the surface of the ground and the antenna (**D**). The sample received signal, shown in Fig. 1, which is for a perfectly electrical conducting (PEC) Vee over a PEC ground plane illustrates the problem that clutter can present.

First, parameters critical to the land mine detection problem are discussed. Parameters characterizing a typical antipersonnel land mine are described, e.g., size and physical composition. Next, the composition and electrical parameters of the ground (soil) are discussed and representative cases are selected. Then, a simple one-dimensional (1-D) analysis is performed to guide the selection of the shape and duration of the radiated pulse.

Details of implementing a fully three-dimensional (3-D) finite-difference time-domain (FDTD) model to simulate the GPR problem, shown in Fig. 1, are then discussed. This includes modeling the antenna, air, soil, and land mine. To limit the computational requirements, an absorbing boundary condition is placed around the working volume. This model is used to evaluate and select a resistively loaded Vee dipole for further study.

Finally, results obtained with the fully 3-D FDTD model for the GPR land mine detection problem are presented. Parametric studies related to the problem include: varying the height of the Vee above the ground, varying the position of the land mine both laterally and in depth, and examining the effects of the geometry of the land mine on the received signal. Also, environmental conditions are examined including signal returns from rocks and variations in the shape of the surface of the ground. The FDTD results are validated by comparisons with experimental data.

II. Parameters for the Antipersonnel Land Mine GPR

Some parameters associated with using a short-pulse GPR to detect small antipersonnel land mines buried in the ground (soil) can be chosen, e.g., parameters for the radiated pulse and antenna; others are fixed or beyond control, e.g., properties of the land mine and soil. In studying this problem, it is important to select parameters that realistically model typical conditions.

Descriptions of some land mines are contained in [5]–[7]. The Italian TS-50 and VS-50 land mines were selected as representative models of antipersonnel land mines for this study. They are nonmetallic and rotationally symmetric (neglecting some small fins) with a cylindrical base (diameter of 8 cm and height of 3.2 cm) and a cylindrical plunger/trigger on top (diameter of 4 cm and height of 1 cm). Typically, they are deployed at depths ranging from 0 to 2 cm. In general, antipersonnel land mines can be effectively deployed at depths ranging up to about 10 cm.

For the FDTD numerical studies, two models are used to simulate small antipersonnel land mines. First, a simple cylindrical land mine with a height of 3.2 cm and diameter of 8 cm (similar to the base of the TS-50 and VS-50 land mines) is used in some of the parametric studies. Where a more realistic model is desired, a typical land mine is modeled as a stack of two dielectric cylinders with the dimensions based on the TS-50 and VS-50 land mines. The electrical parameters selected to model the land mines are $\epsilon_r = 3$, $\sigma = 0$, and $\mu = \mu_0$, which are typical for plastics and explosives.

The composition and electrical parameters of the soil play a critical role in detection as they affect the size and shape of the return(s) from the land mine. Soils are a mixture of soil particles, air voids, and water, with electrical parameters (conductivity and permittivity) that vary greatly with soil density, water content, soil texture (e.g., sand, silt, and clay) and frequency of operation (dispersion). This makes it difficult to select parameters to realistically model all the conditions that can be encountered. Here, the soils are assumed to be nonmagnetic $\mu = \mu_0$.

Based on measurements reported in the literature [8]–[11], three full soil models are selected as representative of a variety of soils. The frequency dependence of the electrical parameters of soils is mainly due to the water content. Therefore, the frequency dependence of the effective relative permittivity and effective conductivity are modeled with the Debye formula [9] as

$$\epsilon_{re} = \epsilon_{r\infty} + \frac{\epsilon_{rs} - \epsilon_{r\infty}}{1 + \omega^2\tau^2} \tag{1}$$

and

$$\sigma_e = \sigma_0 + \frac{\epsilon_{rs} - \epsilon_{r\infty}}{1 + \omega^2\tau^2}\ \omega^2\tau\epsilon_0 \tag{2}$$

where σ_0 and ϵ_{rs} are the low-frequency conductivity and relative permittivity, $\epsilon_{r\infty}$ is the high-frequency relative permittivity, and τ is the relaxation time. A relaxation time of 9 ps was selected based on τ for water at room temperature (70°F or 21.1 °C) [10]. The corresponding relaxation frequency is $f_m = 1/(2\pi\tau) = 17.7$ GHz. The remaining parameters were selected to match the electrical properties of soils measured at lower frequencies. The soil parameters (shown in Table I) represent dry (about 5% water content by dry soil weight), medium (about 10%), and wet (about 20%) soils. Plots of ϵ_{re} and σ_e for these soils based on (1) and (2) are shown in Fig. 2.

III. Pulse Parameters

A simple analysis was performed to estimate the radiated pulse that will be most effective for a GPR used to detect small land mines buried under a layer of soil. The selection of a differentiated Gaussian (DFG) pulse with a spectral peak at 4 GHz as the radiated pulse involved some tradeoffs. In order to resolve the physical features of the land mine, the pulse should be as short in duration as possible, i.e., higher frequencies. However, while the effective relative permittivity and effective conductivity are nearly constant at lower frequencies, the conductivity (loss) starts rising rapidly around 1 GHz, as seen in Fig. 2. Therefore, a pulse of longer duration (lower frequencies) will more effectively penetrate the layer of soil. Another issue when selecting the radiated pulse is that the return from the land mine should be much larger than the clutter, e.g., ten or more times greater in magnitude (20 dB) to enable the land mine to be clearly distinguished.

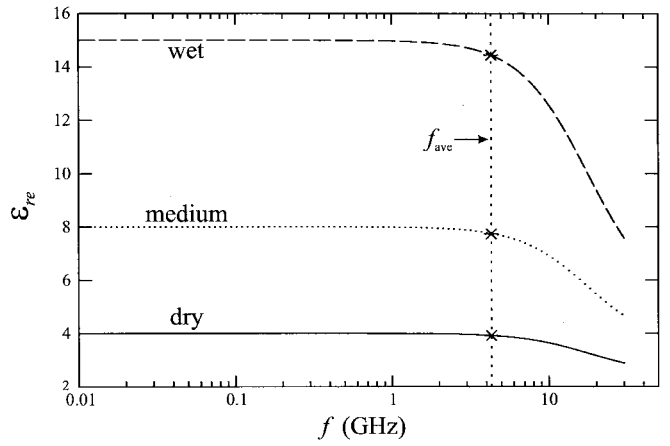

(a)

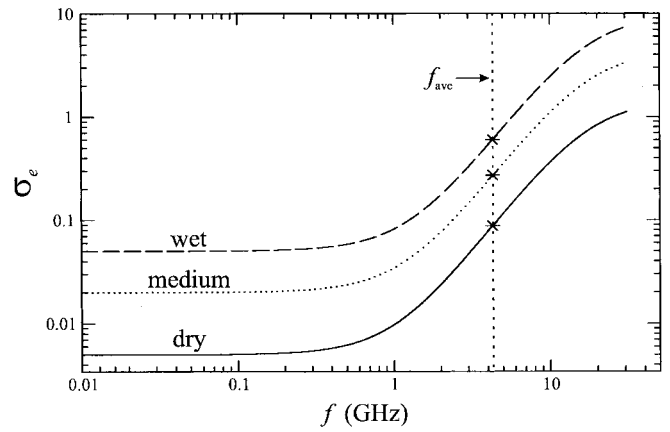

(b)

Fig. 2. (a) Effective relative permittivity and (b) effective conductivity for the dry (solid line), medium (dotted line), and wet (dashed line) soils.

Fig. 3(b) shows a unit-amplitude DFG pulse

$$\mathcal{V}(t) = -(t/\tau_p)\exp[0.5 - 0.5(t/\tau_p)^2] \tag{3}$$

where τ_p is the characteristic time and Fig. 3(c) shows the corresponding normalized frequency spectrum

$$V(f) = (f/f_{\rm pk})\exp[0.5 - 0.5(f/f_{\rm pk})^2] \tag{4}$$

where $f_{\rm pk} = 1/(2\pi\tau_p)$ is the frequency of the spectral peak. Some reasons for selecting a DFG pulse are: no zero-frequency component, a well defined spectral peak, and negligible spectral content for frequencies above about $3.5f_{\rm pk}$. A signal similar to a DFG pulse is radiated when a Gaussian pulse

$$\mathcal{V}(t) = \mathcal{V}_0\exp[-0.5(t/\tau_p)^2] \tag{5}$$

is used to drive the antenna; Vee antennas radiate a signal that is roughly the derivative of the input.

To estimate the performance of the GPR, the simple layered model of a land mine buried in soil with a normally incident plane wave, shown in Fig. 3(a), was used. The model consists of an upper soil layer over a mine layer which, in turn, is over a soil layer of infinite thickness. For an antenna which radiates a pulse into a small spot on the surface of the ground, this is a reasonable model for evaluating how DFG pulses of varying length interact with the soil and land mine. The upper soil layer was $d_S = 2$ cm thick, the maximum typical deployment depth of the TS-50 and VS-50 land mines. The mine layer was $d_M = 3.2$ cm thick, similar to the base of these land mines. The electrical parameters discussed in the previous section were used for the land mine and soil.

First, some comparisons are made in the frequency domain. The reflection coefficient at the surface of the ground (air-soil interface) is

$$\Gamma_{\rm surf} = \frac{\eta_S - \eta_0}{\eta_S + \eta_0} \tag{6}$$

where $\eta_0 = \sqrt{\mu_0/\epsilon_0}$ and $\eta_S = \omega\mu_0/k_S$ are the intrinsic impedances of free space and the soil, respectively. The wave number k_S for the soil is

$$k_S = \omega\sqrt{\mu_0\epsilon_S} = \frac{\omega}{c}\sqrt{\epsilon_{re}}\sqrt{1 - j\frac{\sigma_e}{\epsilon_{re}\epsilon_0\omega}} \tag{7}$$

where ϵ_{re} and σ_e are calculated using (1) and (2). $|\Gamma_{\rm surf}|$ is relatively independent of frequency except at very low frequencies where there is nearly total reflection. Next, the reflection from only the top surface of the land mine is important as it is indicative of the first (usually largest) return from the buried land mine. This reflection is given by

$$\Gamma_{\rm top} = \tau_{AS}\tau_{SA}\Gamma_{SM}\exp(-j2k_S d_S) \tag{8}$$

where $\tau_{AS} = 2\eta_S/(\eta_0 + \eta_S)$ and $\tau_{SA} = 2\eta_0/(\eta_0 + \eta_S)$ are the transmission coefficients from air into soil and soil into air, respectively, and $\Gamma_{SM} = (\eta_M - \eta_S)/(\eta_M + \eta_S)$ is the reflection coefficient for the soil-mine interface. The intrinsic impedance of the land mine (a simple, lossless dielectric) is $\eta_M = \sqrt{\mu_0/\epsilon_M}$.

Fig. 4 shows the ratio of the reflection from the top surface of the land mine to that from the surface of the ground $|\Gamma_{\rm top}/\Gamma_{\rm surf}|$ versus frequency. Notice that this ratio is nearly the same $|\Gamma_{\rm top}/\Gamma_{\rm surf}| \approx -18$ dB for the three soils when $f = 4$ GHz. An antenna design is needed where the clutter is much smaller than the return from the land mine, a typical value being -20 dB. Hence, for operation near 4 GHz, the clutter should be at least 38 dB below the reflection from the surface of the ground, $\Gamma_{\rm surf}$, as shown in Fig. 4.

A similar study was made in the time domain. Here, a unit-amplitude DFG plane wave (3) is normally incident on the surface of the soil in Fig. 3. The total reflected signal is found by performing an inverse Fourier transform of the product of the spectrum of the incident signal with the reflection coefficient

$$\Gamma = \frac{Z_{\rm surf} - \eta_0}{Z_{\rm surf} + \eta_0} \tag{9}$$

where

$$Z_{\rm surf} = \eta_S\frac{Z_M\cos(k_S d_S) + j\eta_S\sin(k_S d_S)}{\eta_S\cos(k_S d_S) + jZ_M\sin(k_S d_S)} \tag{10}$$

$$Z_M = \eta_M\frac{\eta_S\cos(k_M d_M) + j\eta_M\sin(k_M d_M)}{\eta_M\cos(k_M d_M) + j\eta_S\sin(k_m d_m)} \tag{11}$$

and $k_M = \omega\sqrt{\mu_0\epsilon_M}$ is the wave number in the land mine.

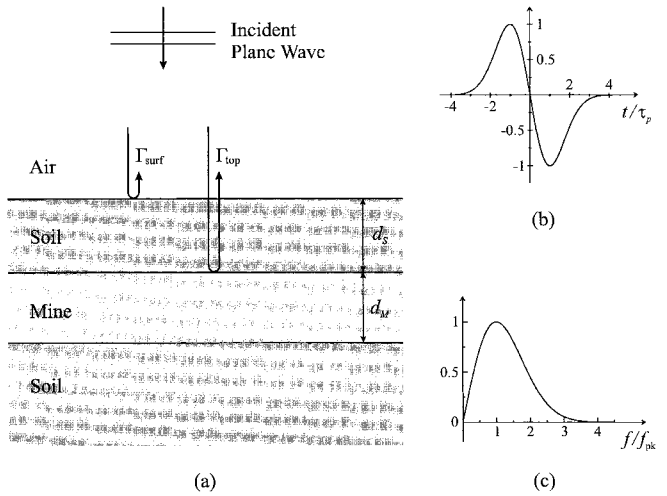

Fig. 3. (a) Simple layered model of a land mine buried in soil with a plane wave normally incident from above. (b) DFG pulse. (c) Corresponding normalized frequency spectrum.

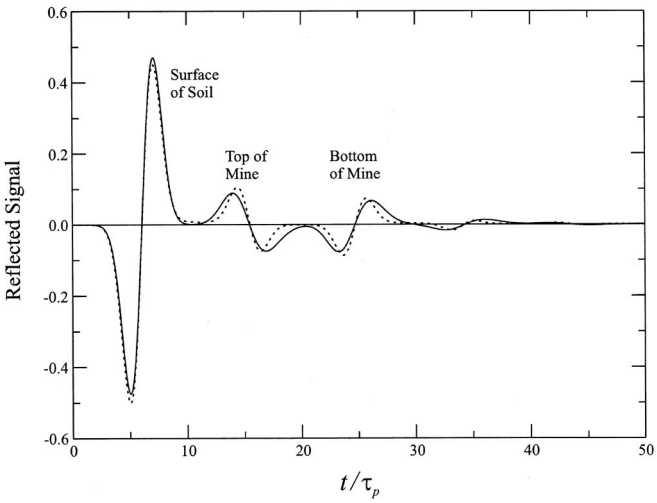

Fig. 5. Pulse reflected from simple layered model of the medium soil containing a 3.2-cm-thick land mine layer buried at a depth of 2 cm using the full (solid line) and simple (dotted line) soil models.

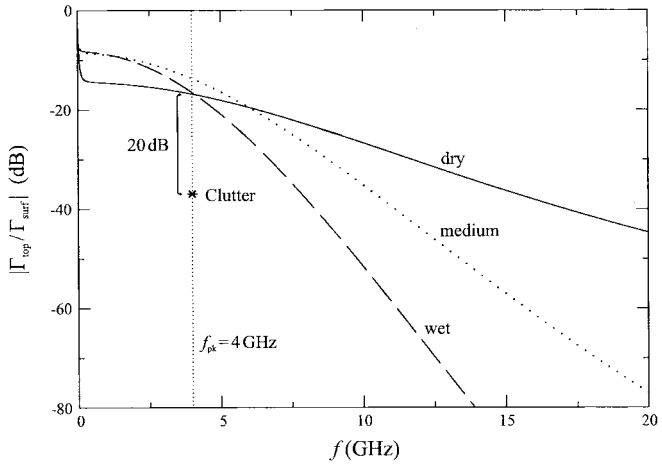

Fig. 4. Magnitude of ratio of the reflection from the top surface of a 3.2-cm-thick land mine layer buried at a depth of 2 cm to the reflection from the surface of the dry (solid line), medium (dotted line), and wet (dashed line) soils.

TABLE I
ELECTRICAL PARAMETERS FOR FULL AND SIMPLE* MODELS OF REPRESENTATIVE SOILS

	Full				Simple	
Soil Type	ϵ_{rs}	$\epsilon_{r\infty}$	σ_0 (S/m)	τ (ps)	ϵ_{re}	σ_e (S/m)
Dry	4	2.5	0.005	9	3.91	0.0892
Medium	8	3.5	0.02	9	7.74	0.273
Wet	15	5	0.05	9	14.4	0.611

* Simple model assumes frequency independent parameters equal to those of full model at $f_{ave} = 4.3$ GHz.

The solid line in Fig. 5 shows the reflected signal from the land mine buried at a depth of 2 cm in the medium soil for an incident DFG signal with a peak frequency of $f_{pk} = 4$ GHz. As shown, a relatively large reflection from the surface of the soil is followed by smaller pulses reflected from the top and bottom surfaces of the land mine layer.

Also shown in Fig. 5 are results for a simple model for the soil (dotted line). The simple soil model uses fixed values for ϵ_{re} and σ_e (see Table I and Fig. 2). These fixed values were selected by evaluating (1) and (2) at the frequency f_{ave}, where 50% of the energy in the pulse is above and 50% below this frequency. For a DFG pulse, $f_{ave} = 1.0879 f_{pk}$. As shown, the reflection from the surface of the simple model of the soil is in good agreement with the full model. The peak-to-peak magnitude of the reflections from the top and bottom surfaces of the land mine predicted by the simple model agree well with the full model. The simple model provided adequate results (within 1 dB) for a DFG pulse with $f_{pk} = 4$ GHz for all of the soils.

Another factor to consider in selecting the DFG pulse is the resolution of the target, i.e., can the signals from the top and bottom surfaces of the land mine be distinguished? It should be recognized that the reflection from the top surface of the land mine can overlap (in time) the reflection from the surface of the soil when the land mine is buried at very shallow depths. For a simple layer model (Fig. 3), a formula can be developed to quantify the resolution of the top and bottom surfaces of a land mine for a given pulse and soil [12, ch. 2]. Once the resolution is greater than 20 dB, the reflections from the top and bottom surfaces of the land mine are effectively resolved. However, since factors such as dispersion, depth of the land mine, and the surrounding environment can decrease the resolution, the DFG pulse should be as short in duration as feasible.

Based on the preceding discussion, a DFG pulse with $\tau_p = 39.8$ ps ($f_{pk} = 4$ GHz) was chosen. This pulse is short enough to provide good resolution of the land mine and long enough for adequate penetration into the representative soils. For this pulse, the ratio of the reflection from the top surface of the land mine to that from the surface of the ground is about -18 dB in the time-domain, indicating that an antenna

design where the clutter is down by about 38 dB from the surface reflection is needed. This requirement can be fulfilled by using resistively loaded Vee dipoles.

IV. FDTD Modeling

A. General

To model a GPR system involving Vee dipole(s) in the air over a simulated ground containing targets (see Fig. 1), the FDTD method was selected. The FDTD method, proposed by Yee [13], is a way of directly computing both the electric and magnetic fields in the time domain. As both the electric and magnetic fields are computed, it is very flexible in modeling materials with varying electrical properties and geometries. Recently, the FDTD method has risen in prominence with advances in computers as evidenced by the large number of publications [14]. Good sources for an introduction to the FDTD method are the books by Kunz and Luebbers [15] and Taflove [16].

The update equations for the six vector field components ($\mathcal{E}_x$, $\mathcal{E}_y$, $\mathcal{E}_z$, $\mathcal{H}_x$, $\mathcal{H}_y$, and $\mathcal{H}_z$ in Cartesian coordinates) computed for the fully 3-D FDTD method can be found in [16, ch. 3]. The materials modeled are simple, lossless, and lossy dielectrics with $\mu = \mu_0$. These update equations are sufficient to model the portions of the computational volume that are completely within the air, soil, and land mine. Modifications are made to the update equations at the interfaces between these regions and for modeling the antennas. To model the air-soil and land mine-soil interfaces, the electric field update equations are slightly modified. In these update equations, the relative permittivity ϵ_r and conductivity σ are replaced with the average relative permittivity $\overline{\epsilon}_r$ and conductivity $\overline{\sigma}$, as calculated over the cell areas for $\mathcal{E}_x$, $\mathcal{E}_y$, and $\mathcal{E}_z$. No modifications are required for the magnetic field updates. The tangential electric field components $\mathcal{E}_x$ and $\mathcal{E}_y$ are placed at the air-soil interface.

Cubic FDTD cells with side lengths of $\Delta = \Delta x = \Delta y = \Delta z$ were used throughout the computational volume. There were at least eight to ten cells per wavelength in the soil at the highest frequency of interest $f_{\max}$, the frequency where the signal power has dropped to a negligible level. A value of $f_{\max}$ where the spectrum is down to 1% (-40 dB) of its peak was deemed sufficient. For numerical stability, the time step Δt should meet the Courant condition, $\Delta t \leq \Delta/(\sqrt{3}v)$, where v is the speed of light in the medium. For convenience, $\Delta t = \Delta/(2c)$ was chosen. For this Δt, it takes two time steps to travel one spatial step in free-space. This allows a very simple absorbing boundary condition to be used with the feeding transmission line [22].

The working volume for the fully 3-D FDTD simulations must be finite. Therefore, an absorbing boundary condition (ABC) is placed around the regular FDTD grid that models the working volume. Recently, the perfectly matched layer (PML) ABC, which splits the electric and magnetic field components, was proposed by Bérenger [17]. It is several orders of magnitude less reflective than previous ABC's. More recently, an anisotropic PML ABC for the 3-D FDTD method was introduced by Sacks *et al.* [18] and further developed by Gedney [19], [20]. The anisotropic PML has the advantage that the field components are not split (less computer memory) while giving equal performance.

For the anisotropic PML ABC selected, the nonphysical electric and magnetic conductivities, σ_i ($i = x$, y, or z), vary with depth into the PML in the i direction (normal to the PML-working volume interface) to avoid a large discontinuity at the interface, while remaining constant in the tangential directions. The selected spatial variation in σ_i is a polynomial taper (smallest at interface). Gedney determined that a fourth-order polynomial yields the best results and found an optimal maximum conductivity $\sigma_{\max}$. A single value of $\sigma_{\max}$ is necessary for stability, even when multiple materials are terminated by the PML, e.g., air and soil. It was shown in [19]–[21] that the reflection error is relatively constant for a range of values greater than the optimal value of $\sigma_{\max}$ before reflections resulting from discretization become significant. Therefore, the largest value of $\sigma_{\max}$, where the PML is adjacent to air, was selected. Based on the results in [19]–[21], a PML that is ten cells thick was used.

B. FDTD Modeling of Antennas

In the fully 3-D FDTD model [see Fig. 1(a)], the resistively loaded Vee dipole is modeled as thin triangular-shaped conductive sheets attached to a feeding 1-D transmission line by thin PEC tabs.[1] The tabs, which connect the arms to the feed, are modeled by simply setting the electric field components to zero in the appropriate locations. The 1-D transmission line is described in [22]. A connection is made between the end-voltage and current nodes of the 1-D transmission line and the electric and magnetic fields of the 3-D FDTD grid at and adjacent to the antenna feed. The electric field in the feed gap $\mathcal{E}_{x,\,\mathrm{gap}}$ is related to the end-voltage node $\mathcal{V}_{\mathrm{end}}$ by

$$\mathcal{E}_{x,\,\mathrm{gap}} = -\mathcal{V}_{\mathrm{end}}/\Delta x \tag{12}$$

where the spacing between the metal tabs of the arms of the dipole is Δx. The last current node in the 1-D transmission line is updated by applying the integral form of Ampere's law to the magnetic field components on a contour surrounding the feed gap.

To achieve the linearly tapered conductivity profile described by

$$\sigma(s/h) = \sigma_0(1 - s/h) \tag{13}$$

the arms of the resistively loaded Vee dipole have a width that varies linearly with the fractional distance s/h along the arms [see Fig. 1(a)] as

$$W(s/h) = W_0(1 - s/h) \tag{14}$$

where $W_0 = 1/(\sigma_{\mathrm{Vee}} d_{\mathrm{Vee}} R_0)$. Here, σ_{Vee} and d_{Vee} are the conductivity and thickness of the sheets composing the arms of the resistively loaded Vee and R_0 is the starting (at $s/h = 0$) value of the resistance per unit length. The feed, which includes the feed gap and part of the metal tabs, has a width of W_{FD}.

[1] This model is based on the experimental antenna discussed later.

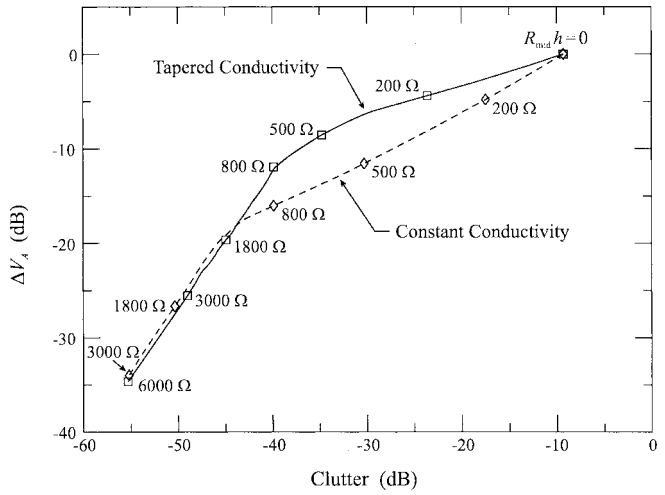

Fig. 6. Peak-to-peak voltage ΔV_A of the initial reflection from a PEC ground plane versus the clutter, maximum peak-to-peak $\Delta V_{B,C}$ or $_D$ divided by ΔV_A for Vee dipoles with tapered and constant conductivity. ΔV_A is normalized by ΔV_A, for the PEC Vee. The Vee antennas ($\alpha = 62^\circ$ and $h = 10$ cm) were 5 cm over the ground plane.

The conductive sheets forming the arms of the resistively loaded Vee dipole are placed in the x–z plane that contains the $\mathcal{E}_x$ and $\mathcal{E}_z$ field components. Some assumptions are made in the FDTD modeling of this antenna. First, the normal electric field component $\mathcal{E}_y$ is assumed to be negligible within the arms. This assumption readily follows from the symmetry of the resistively loaded Vee dipole and the manner in which it is fed. Also, the thickness of the conductive sheets is assumed to be much less than a skin depth at the frequencies of interest. Therefore, $\mathcal{E}_x$ and $\mathcal{E}_z$ are constant within the arms in the direction normal to the plane of the Vee. With these assumptions, the arms can be modeled using the standard FDTD update equations for the magnetic field components and $\mathcal{E}_y$. The update equations for $\mathcal{E}_x$ and $\mathcal{E}_z$ are modified by replacing the relative permittivity ϵ_r and conductivity σ with the average relative permittivity $\overline{\epsilon}_r$ and conductivity $\overline{\sigma}$ as calculated over the appropriate cell areas.

C. Resistive Antenna Selection

An initial study of Vee dipoles with resistive loading was made to show they can achieve higher gains and lower levels of clutter than comparable linear dipoles [3], [4]. A method of moments (MoM) program (the numerical electromagnetics code or NEC) was used to study these antennas in free-space and over a perfectly conducting ground. The antennas were modeled as having thin cylindrical arms. Two types of resistively loaded antennas were considered, one with constant conductivity and one where the conductivity is tapered as in (13). The quantity $R_{\rm mid}h$ is convenient for comparing the various resistively loaded designs. It is the resistance per unit length at the midpoint of an arm multiplied by the length of the arm. $R_{\rm mid}h = 2R_0h$ for the tapered conductivity design, and $R_{\rm mid}h = R_0h$ for the constant conductivity design.

In Fig. 6, the peak-to-peak difference voltage due to the initial reflection of the radiated pulse from the PEC ground plane ΔV_A (normalized by ΔV_A for a PEC Vee) is plotted versus the clutter as a function of $R_{\rm mid}h$. The difference voltage is the portion of the voltage in the feeding transmission line caused by the presence of the PEC ground plane. It is calculated by subtracting the voltage in the feeding transmission line for the antenna in free space from the voltage when the antenna is over the PEC ground. The clutter is the maximum peak-to-peak value of signals $\mathbf{B}$, $\mathbf{C}$, and $\mathbf{D}$ in Fig. 1 divided by ΔV_A. ΔV_A is indicative of the size of the radiated pulse and, hence, the size of the return from a buried land mine. Ideally, ΔV_A should be as large as possible and the clutter should be as small as possible. Both resistively loaded designs reduced the desired signal (ΔV_A) as well as the clutter relative to PEC Vee dipoles (see Fig. 6). For a clutter reduction of -38 dB, the tapered conductivity design is preferable, because it returns a larger signal ΔV_A than the constant conductivity design for the same level of clutter.

For the FDTD study, a resistively loaded Vee dipole made with thin-sheet conductive arms, where the width of the arms varies as given by (14) was used. The characteristic impedance Z_0 (real) of the feeding transmission line for each antenna was selected to minimize clutter. At a single frequency, it can be shown that the reflection coefficient Γ at the feed of the antenna is minimized when $Z_0 = |Z_{\rm in}|$ where $Z_{\rm in}$ is the input impedance of the antenna. Z_0 was selected to be $|Z_{\rm in}|$ at $f_{\rm pk}/2$ where $f_{\rm pk}$ is the frequency at the peak of spectrum of the radiated electric field at boresight. This value is an average selected to minimize the reflection at the feed for the excitation (a Gaussian pulse) and the initial reflection from the ground (a DFG pulse), the major sources of clutter. It was verified that this design performs in a manner similar to the cylindrical antennas in the earlier MoM study.

The interior angle α and arm length h were selected so that the Vee has an aperture (distance between the open ends of the arms) that is roughly equivalent to the diameter of typical antipersonnel land mines. The spot illuminated on the ground is roughly the size of the aperture at close distances [4]. Another consideration is that the arms be long enough to allow the resistive loading to attenuate the pulse sufficiently before it reaches the open end of the antenna (reduce clutter). Typically, h must be at least three pulse lengths to meet this requirement, and the ratio of τ_p for the Gaussian pulse to the antenna transit time $\tau_a = h/c$ should be $\tau_p/\tau_a \leq 0.07767$. τ_p is selected to ensure the Vee radiates a signal similar in shape to a DFG pulse with $f_{\rm pk} = 4$ GHz.

The resistively loaded Vee selected had dimensions of $\alpha = 43.6^\circ$ $h = 10.85$ cm and $W_{\rm FD} = 3$ mm. These dimensions result in an aperture of 8.36 cm, roughly the diameter of the TS-50 and VS-50 land mines. For the thin-sheet design, the clutter drops rapidly with increasing resistive loading before the rate of decline begins to level-off in a manner similar to Fig. 6. The tapered resistively loaded Vee had arms where $R_{\rm mid}h = 800\ \Omega$ with $d_{\rm Vee} = 0.48$ mm, $\sigma_{\rm Vee} = 125$ S/m, $W_0 = 4.52$ mm, and $\epsilon_r = 3$. This design reduces the clutter by about 38 dB with respect to a comparable PEC antenna over a PEC ground plane (worst-case scenario); this meets the criteria developed using the layered model. To radiate a DFG pulse with $f_{\rm pk} = 4$ GHz, the antenna is driven with a Gaussian pulse (5) with $\tau_p = 28$ ps ($\tau_p/\tau_a = 0.0774$) by a

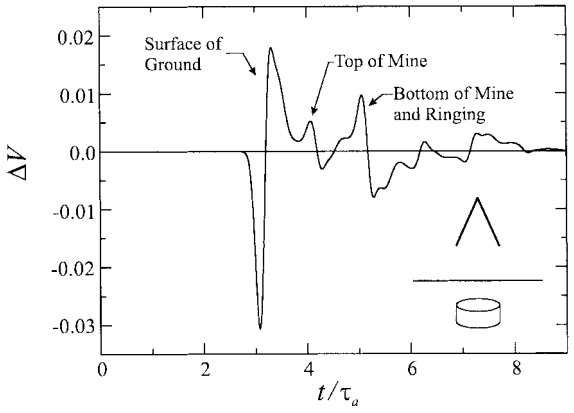

(a)

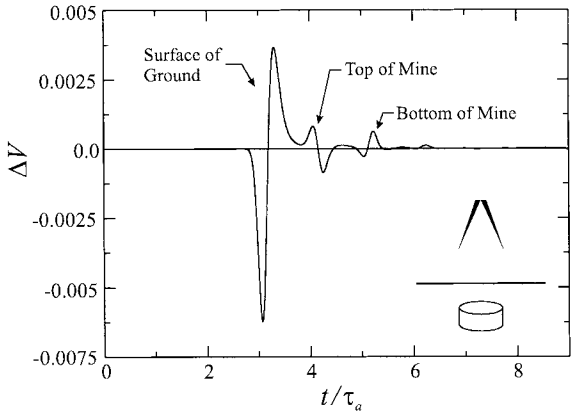

(b)

Fig. 7. Difference voltages for (a) PEC Vee and (b) resistively loaded Vee dipoles centered at a height of 4 cm over the medium soil containing the simple cylindrical land mine buried at a depth of 2 cm.

250-Ω transmission line. For the simulations, the Vee antennas were driven by a unit-amplitude Gaussian pulse.

Fig. 7 shows the difference voltages for the resistively loaded Vee and a comparable PEC Vee centered 4 cm over the surface of the medium soil containing the simple cylindrical land mine buried at a depth of 2 cm. For the PEC Vee, the initial return from the bottom surface of the land mine is completely obscured by the clutter, as shown in Fig. 7(a). However, as shown in Fig. 7(b), the initial returns from the top and bottom surfaces of the land mine are visible for the resistively loaded Vee dipole. Clearly, the resistively loaded Vee makes the task of distinguishing a buried land mine from clutter much easier.

V. Parametric Studies

In this section, parametric studies are conducted on the resistively loaded Vee dipole in the air over a simulated ground containing a land mine, see Fig. 1. The parametric studies include varying the height of the antenna over the ground, the depth and relative position of the land mine, and the profile of the land mine. Unless otherwise stated, the simple cylindrical land mine model was used. The soils are modeled as lossy dielectrics using the simple model (see Table I). It should be

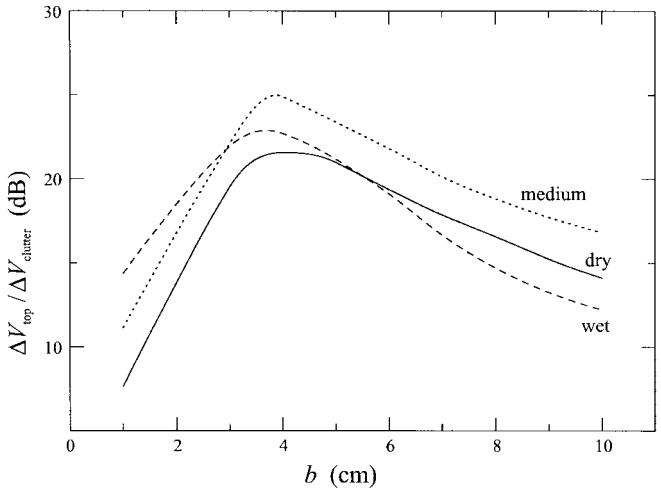

Fig. 8. Ratio of the peak-to-peak difference voltage caused by the top surface of the simple cylindrical land mine to the clutter for the dry (solid line), medium (dot line), and wet (dashed line) soils for the resistively loaded Vee dipole placed at varying heights b.

emphasized that the goal of this research is to develop and study antennas that are suitable for a short-pulse GPR, not land mine/target identification or signal processing.

First, the resistively loaded Vee dipole was placed at varying heights b above the ground in which the land mine was buried at a depth of 2 cm. The height is of particular interest as it can be controlled, unlike the properties of the ground and target(s). As expected, the magnitude of ΔV decreases as b increases. While varying b, heights were found that minimized clutter. Fig. 8 shows the ratio of the peak-to-peak difference voltage caused by the top surface of the land mine $\Delta V_{\rm top}$ to the peak-to-peak difference voltage caused by clutter $\Delta V_{\rm clutter}$ as a function of the height of the antenna above the ground. Recall that the clutter does not include the direct reflection from the surface of the ground, $\mathbf{A}$ in Fig. 1. $\Delta V_{\rm top}$ was selected as it has the largest peak-to-peak magnitude. The criteria that $\Delta V_{\rm top}/\Delta V_{\rm clutter} \geq 20$ dB is satisfied for the three soils at heights ranging from 3 cm to 5.5 cm. A peak in $\Delta V_{\rm top}/\Delta V_{\rm clutter}$ occurs near $b = 4$ cm for all three soils due to clutter signals partially canceling one another. Based on these results, an antenna height of $b = 4$ cm will be used for the remainder of the parametric tests.

Next, the effect of the depth of the land mine on the shape and magnitude of the return from the land mine are examined. Fig. 9 shows the difference voltage for the resistively loaded Vee dipole centered over the simple cylindrical land mine buried at varying depths d_S in the medium soil. When the land mine is flush with the surface $d_S = 0$, the return from the surface of the ground is the return from the top surface of the land mine; the subsequent pulse is caused by the bottom surface. As the land mine is placed at increasing depths, the return from the top of the land mine separates from the return from the surface of the ground. However, the spacing (in time) between the returns from the top and bottom surfaces of the land mine remains constant. The returns from the land mine become smaller as the depth of the land mine increases due to

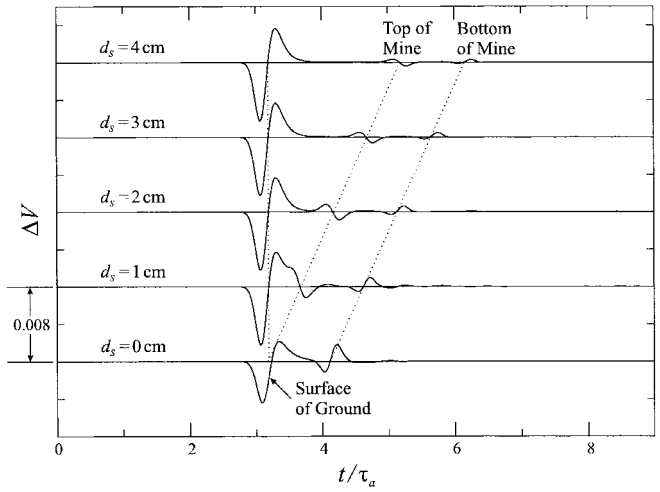

Fig. 9. Difference voltage for the resistively loaded Vee dipole at a height of 4 cm over the medium soil containing the simple cylindrical land mine buried at varying depths d_S.

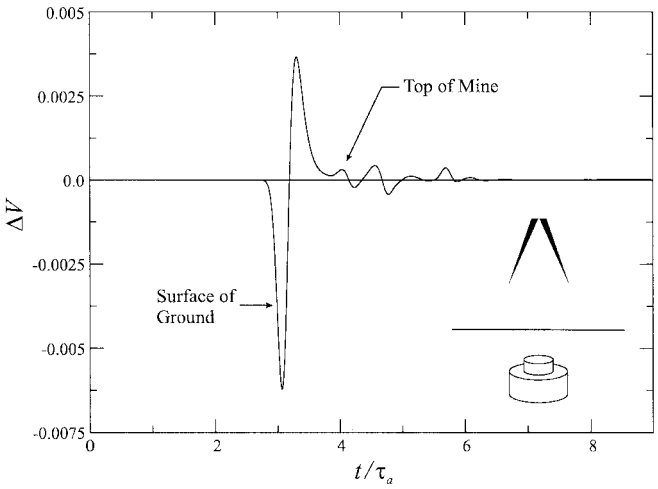

Fig. 10. Difference voltage for the resistively loaded Vee dipole centered at a height of 4 cm over the medium soil containing the typical land mine buried at a depth of 2 cm. Compare with Fig. 7(b) for the simple land mine under the same conditions.

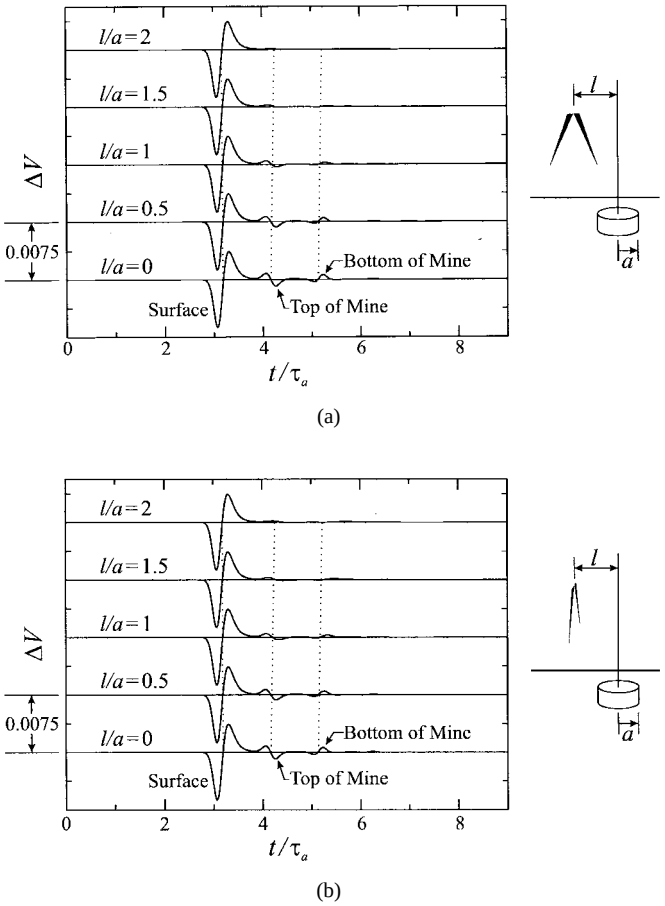

Fig. 11. Difference voltage for the resistively loaded Vee dipole at a height of 4 cm over the medium soil containing the simple cylindrical land mine at a depth of 2 cm at varying distances in (a) the plane of the Vee and (b) the plane perpendicular to the plane of the Vee.

losses in the soil as well as the land mine being illuminated by a smaller portion of the radiated wavefront. As would be expected for a soil modeled as a simple lossy dielectric, once the land mine is completely buried, ΔV decreases nearly exponentially as d_S increases (straight line on a decibel scale).

The effect of the geometry or profile of the land mine on the size and shape of the return was also examined. Two land mine profiles are studied, the simple cylindrical land mine and the typical land mine (patterned after the TS-50 and VS-50 land mines). ΔV for the resistively loaded Vee dipole centered over the simple and typical land mines buried at a depth of 2 cm in the medium soil are shown in Figs. 7(b) and 10, respectively. The returns from the top and bottom surfaces of the simple cylindrical land mine are readily distinguished; however, the return from the typical land mine is more complex. The return from the topmost surface of the typical land mine is followed by a return from the horizontal surface 1 cm lower. Depending on the soil (differing velocities of propagation), these returns overlap in different fashions. In addition, there are the returns from the bottom of the land mine caused by the portions of the signal that penetrated the two upper horizontal surfaces. The time delays for these signals, which propagate inside the land mine, are independent of the properties of the surrounding soil. This can be used to develop "signatures" to identify land mines, a major research topic in its own right.

The effect of the relative positions of the antenna and land mine is the last item addressed. Here, the position of the simple cylindrical land mine is varied in the plane of the Vee and perpendicular to the plane of the Vee. Fig. 11 shows ΔV for $0 \leq l/a \leq 2$ where l is the distance from the axis of symmetry of the Vee to the axis of symmetry of the land mine and a is the radius of the land mine. The ground is the medium soil and the land mine is buried at a depth of 2 cm. The returns from the top and bottom surfaces of the land mine are largest when the antenna is centered over the land mine ($l/a = 0$) and decrease as l/a increases. Interestingly, the time delay between the return from the surface of the ground and the land mine increases more slowly than might be expected. However, an examination of the roundtrip path length for a spherical wave traveling between the feed of the antenna and the land mine confirms that the time delays are correct.

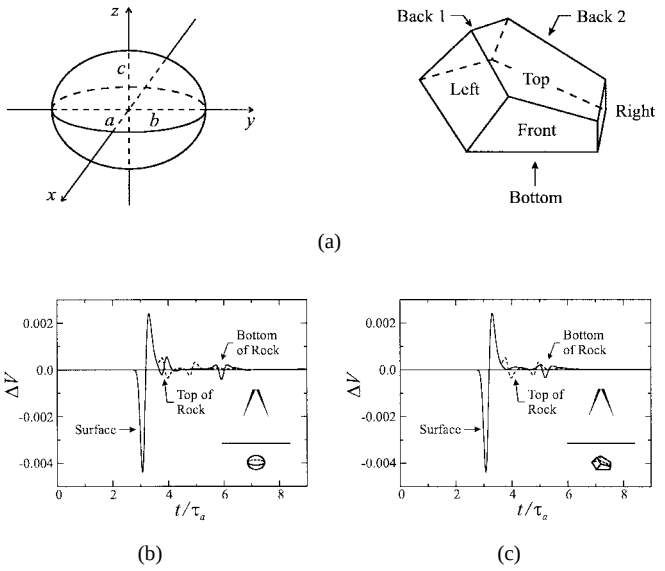

Fig. 12. (a) Ellipsoid and polyhedron used to model rounded and jagged rocks. Difference voltage (solid line) for medium-sized (b) rounded and (c) jagged rocks buried at a depth of 2 cm in the dry soil. The return from the simple cylindrical land mine buried at a depth of 2 cm under a flat ground surface is shown for comparison (dashed line).

VI. Environmental Conditions

Environmental conditions can adversely affect the performance of a short-pulse GPR. For example, the GPR will detect the presence of buried objects other than land mines, such as pebbles and rocks. This may give rise to false alarms. Also, variations in the surface of the ground can have an effect on the received signal. This section will examine how the resistively loaded Vee antenna performs with regard to buried rocks and variations in the surface of the ground.

First, the returns from rocks are examined. A feldspar (labradorite) was selected for the FDTD simulations. At 4 GHz, feldspar has a relative dielectric constant of $\epsilon_r = 6$ and a conductivity of $\sigma = 0.0173$ S/m [23]. Two different rock shapes were selected as representative of what is found in the field, one was rounded and the other was jagged. As shown in Fig. 12(a), the rounded rock was modeled as an ellipsoid defined by a width $2a$ (x-direction), depth $2b$ (y-direction), and height $2c$ (z-direction). The jagged rock was modeled as a polyhedron defined by seven planes [see Fig. 12(a)]. In the plane of the Vee, the top surface of the jagged rock is at an 18° angle with the surface of the ground while the bottom of the rock is parallel to the surface of the ground. For each rock shape a small, medium, and large size was defined. The small rocks had a maximum dimension about half the size of the aperture of the Vee antenna. The large rocks had a maximum dimension roughly the size of the aperture, while the medium rocks were in between. For example, the medium rounded rock has a width, depth, and height of 5.6 cm, 5.1 cm, and 4.5 cm, respectively.

ΔV for the medium-sized rounded and jagged rocks buried at a depth of 2 cm in the dry soil and centered below the antenna are shown in Fig. 12(b) and (c), respectively, (solid line). For comparison, returns from the simple cylindrical land mine are also shown (dashed line). The returns caused by the rocks are clearly evident in the dry soil, mainly because of the difference in the relative dielectric constant of the rock ($\epsilon_r = 6$) and soil ($\epsilon_r = 3.91$). With the exception of the small-sized rocks, the magnitude of the returns are larger for the rounded rock and comparable for the jagged rock to those caused by the land mine in the dry soil. Regardless of rock size or soil, the returns from the top surface of the jagged rocks were significantly smaller than those from the comparable rounded rocks. This occurs because the top surface of the jagged rock is at an angle with the surface of the ground, reflecting the incident pulse away from the boresight of the antenna.

In the medium soil, the returns from the rocks were much smaller with respect to those from the land mine. In this case, the difference in the relative dielectric constants between the rock ($\epsilon_r = 6$) and medium soil ($\epsilon_r = 7.74$) is much smaller. This points out a potential shortfall of GPR's, that when the target has a relative dielectric constant close to that of the soil, there is little or no return.

When the rocks were placed in the wet soil, the returns from the rounded rocks, while smaller than those caused by the land mine, were clearly evident. An example of the large rounded rock in the wet soil is shown in Fig. 13(a). Note the similarity in the initial returns from the rock and land mine. If this rock had a flat bottom and was similar in thickness to the land mine, it would be difficult to distinguish from the land mine. In this case, the returns caused by the jagged rocks were nearly imperceptible. Here, the difference in the relative dielectric constants between the rock ($\epsilon_r = 6$) and the wet soil ($\epsilon_r = 14.4$) is much larger. However, the contrast between the land mine ($\epsilon_r = 3$) and wet soil is even greater. As demonstrated, this GPR will detect rocks. Therefore, the process of distinguishing returns caused by rocks from those caused by land mines is critical, a topic outside the scope of this study.

Now, the effect of variations in the surface of the ground on the detection of a buried land mine are examined. Because the resistively loaded Vee selected has an aperture of only 8.36 cm, gradual changes in the surface of the ground such as a slope were not considered. Three types of surface variations are considered: a depression, a mound, and surface roughness. The simple cylindrical land mine is buried at a depth of 2 cm in the medium soil. For comparison, the return for the simple cylindrical land mine under a flat surface is also shown.

A depression over the land mine can occur due to settling in the soil over and around the land mine. Here, the depression is centered over the land mine, leaving a minimum of 1 cm of soil over it. Another situation is that soil can be mounded over the land mine, perhaps when the land mine is being deployed displaced soil is put over the land mine. The mound is modeled as the inverse of the depression, i.e., the land mine will have a maximum of 3 cm of soil over it. The depression and mound are modeled as having the Gaussian profile $\exp(-0.5\rho^2/\rho_0^2)$ cm, where ρ is the radial distance from the center and ρ_0 is the characteristic length. The value $\rho_0 = 3.728$ cm gives the depression and mound a diameter of 8 cm when the profile is 10% of the maximum and a maximum depth or height of 1

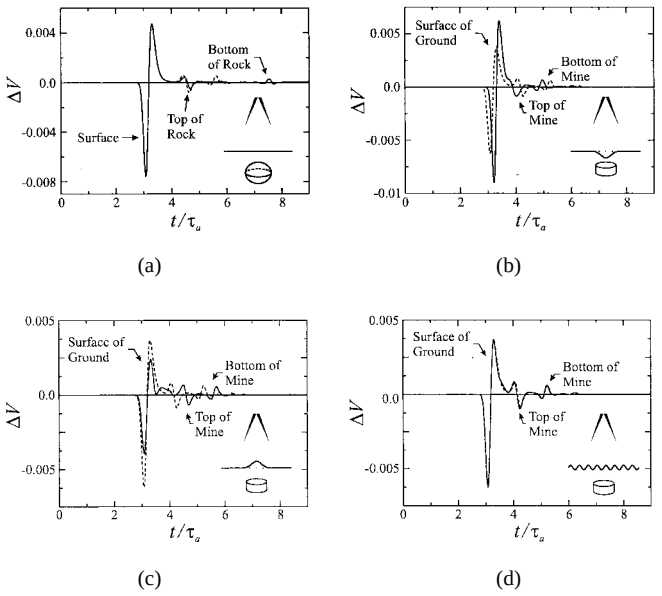

Fig. 13. Difference voltage (solid line) for a (a) large rounded rock buried at a depth of 2 cm in the wet soil, the simple cylindrical land mine buried in the medium soil with (b) a depression or (c) a mound at the surface of the ground centered over it, and (d) furrows in the surface of the ground perpendicular to the plane of the Vee. The return from the simple cylindrical land mine buried at a depth of 2 cm under a flat ground surface is shown for comparison (dashed line).

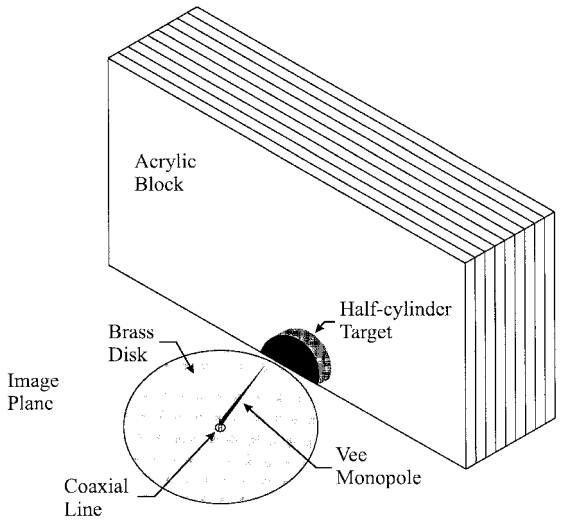

Fig. 14. Experimental model: Vee monopole mounted over image plane with an acrylic block used to simulate the ground.

cm. In Fig. 13(b) and (c), ΔV is shown along with sketches of the depression and mound.

As shown in Fig. 13(b), the reflection from the depression in the ground is significantly larger than that from the flat ground. The depression appears to focus the reflection from the ground back toward the antenna, somewhat like a reflector antenna. Conversely, the reflection from the mound [Fig. 13(c)] is significantly smaller than that from the flat ground; the incident pulse is scattered. In both cases, the returns from the land mine are relatively unchanged in magnitude and shape. Naturally, the time delay between the return from the surface of the soil and that from the land mine is changed, e.g., shorter delay for the depression and longer delay for the mound.

Roughness in the surface of the soil can occur from a variety of causes. Here, it will be assumed that the surface of the soil has been raked, leaving 1-cm-deep furrows in the surface of the soil spaced every 2 cm. Furrows were modeled both parallel and perpendicular to the plane of the Vee. The furrows are modeled as having the sinusoidal shape $0.5\sin(2\pi l/2)$ cm, where l is the distance in the x or y directions in centimeters. ΔV and a sketch of the furrows perpendicular to the plane of the Vee are shown in Fig. 13(d). As shown, the furrows have a minimal effect on the returns. This indicates that roughness in the surface of the ground that is much smaller ($\lesssim$20%) than the Vee aperture or land mine has little effect on the received signal.

VII. Experimental Studies and Validation

The primary purpose of the experiments was to examine the validity of the FDTD models used for the antennas, ground, and land mines. Also, the experiments confirm that resistively loaded Vee antennas reduce clutter with respect to similar PEC Vee antennas.

Monopole Vee antennas were used in the experimental studies. The antenna was attached to the center conductor of an APC-7 connector (50 Ω) mounted at the center of a brass disk fitted into a 6.1 m $\times$ 6.1 m aluminum image plane (see Fig. 14). The arm of the resistively loaded Vee monopole was constructed from conductive, polycarbonate, plastic sheets with $R_{\rm mid}h = 800\,\Omega$. The resistively loaded Vee was built as closely as possible to the specifications in Section IV-C. For comparison, a PEC Vee monopole was built using cylindrical copper wire (24 AWG). The arms of these Vee monopoles were of length $h = 10.85$ cm and at an angle of $\alpha/2 = 21.8°$ to the image plane.

A plastic block was used to simulate the ground in the experiments. It consists of nine, 2.38 $\pm$ 0.05-cm-thick acrylic sheets placed together to form an 81.3 cm wide $\times$ 40.6 cm tall block, see Fig. 14. The acrylic sheets were fastened together by five nylon bolts (not shown) placed near the edges of the block. The electrical parameters of the acrylic at 4 GHz, $\epsilon_r = 2.6$ and $\sigma = 0.003$ S/m, were interpolated from measured values at 3 GHz [24], [25] and 11 GHz [26].

As shown in Fig. 14, one of the acrylic sheets has a half-cylinder slot cut at the center of the bottom edge to allow for the placement of various targets that are similar in shape to the simple cylindrical land mine used in the parametric studies. Since the experimental work is performed on an image plane, the half-cylinder is equivalent to the full cylinder used in the simulations. Five half-cylinder (radius of 4 cm and thickness of 2.38 cm) targets were used: air, aluminum, Teflon, Delrin (acetal), and Stycast.[2] The electrical properties used to model the targets are given in Table II and were taken or interpolated from values in [24]–[26].

The experimental measurements were made with a Hewlett-Packard (HP) 8510C Network Analyzer. The scattering param-

[2]Teflon and Delrin are registered tradenames of E.I. duPont de Nemours & Co. Inc. and Stycast is a registered tradename of Emerson & Cuming, Inc.

TABLE II
ELECTRICAL PARAMETERS FOR THE EXPERIMENTAL TARGETS

Target	ϵ_r	σ (S/m)
Air	1.0	0.0
Aluminum	1.0	3.5×10^7
Teflon	2.1	0.0003
Delrin	2.8	0.006
Stycast	7.0	0.005

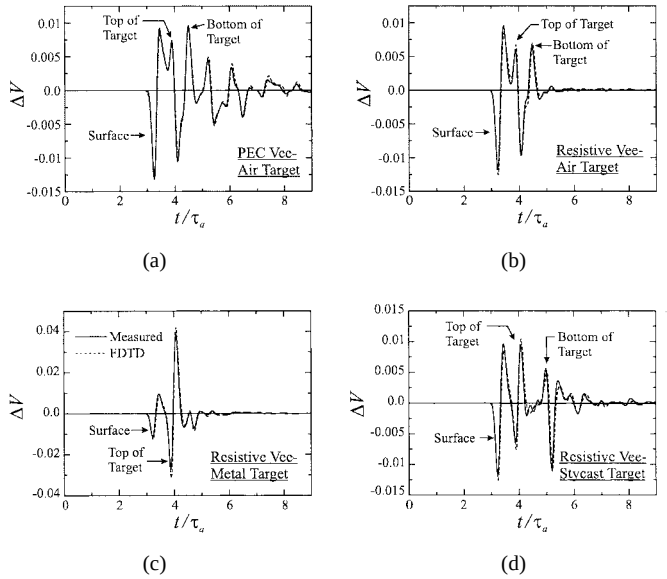

Fig. 15. Measured (solid line) and calculated (dashed line), using the FDTD method, difference voltages for a (a) *PEC Vee dipole* illuminating an air target and a *resistively loaded Vee dipole* illuminating (b) air, (c) Stycast, and (d) aluminum targets. The antennas are centered 5 cm from the acrylic block containing target(s) at a depth of 2.38 cm.

eter S_{11} was measured at 801 equally spaced points within the frequency range of 45 MHz to 18.045 GHz (22.5 MHz intervals). From S_{11}, the input impedance Z_{in} of the antenna was calculated at each frequency. With Z_{in} known, the input reflection coefficient Γ_{in} can be calculated for a transmission line of arbitrary characteristic impedance Z_0' using

$$\Gamma_{\text{in}} = \frac{Z_{\text{in}} - Z_0'}{Z_{\text{in}} + Z_0'}. \tag{15}$$

Now, the reflected voltage in the transmission line can be calculated by an inverse Fourier transform of the product of Γ_{in} and the spectrum of the incident voltage, i.e.,

$$\mathcal{V}_{\text{ref}}(t) = \mathcal{F}^{-1}\{\Gamma_{\text{in}} V_{\text{in}}\} \tag{16}$$

where $V_{\text{in}} = \mathcal{F}\{\mathcal{V}_{\text{in}}(t)\}$.

ΔV caused by reflections from the acrylic block without a target and with the five targets were calculated using the FDTD method as well as measured. A sample of the results is shown in Fig. 15 for the PEC and resistively loaded Vee antennas. Here, the acrylic block was placed 5 cm from the antennas. The surface of the acrylic block was perpendicular to the axis of symmetry of the Vee's. The targets were placed at a depth of 2.38 cm (one sheet) and centered with respect to the axis of symmetry of the Vee antenna. As shown, the ΔV calculated from the measurements and using the FDTD model are in good agreement for both antennas and the various targets. For the PEC Vee, clutter obscures portions of the returns from the targets, e.g., air target in Fig. 15(a). However, the resistively loaded Vee greatly reduced the clutter, e.g., air target in Fig. 15(b), allowing the return from the target to be clearly distinguished. Returns from aluminum and Stycast targets, using the resistively loaded Vee, are shown in Fig. 15(c) and (d), respectively.

In Fig. 15, there are slight differences between the peaks in ΔV for the experimental and FDTD results. In most cases, the FDTD results had higher peaks. The most probable cause is small variations in the alignment of the acrylic block during the experiments, e.g., the surface of the block might not be perfectly normal to the plane of the Vee or exactly 5 cm away. Also, differences in the feeds for the FDTD dipole and experimental monopole have an effect on ΔV.

Other tests included placing the resistively loaded Vee at varying distances from the acrylic block with the Delrin target at a constant depth, varying the depth of the Delrin target inside the acrylic block, and placing the air target at varying positions in the plane perpendicular to the Vee [12]. Also, the resistively loaded and PEC Vees were tested adjacent to a metal plate, i.e., a PEC ground. In all cases, the experimental and FDTD results were in good agreement.

VIII. SUMMARY AND CONCLUSIONS

Using resistively loaded Vee dipoles in a short-pulse GPR to detect small buried antipersonnel land mines was studied using a fully 3-D FDTD model. These antennas, constructed from linearly tapered, thin, conductive sheets, can greatly reduce clutter related to the antenna. This makes the task of distinguishing land mines (targets) much easier. The parametric and environmental studies demonstrated the utility of the antenna developed. An interesting result was that under certain soil and target conditions, the returns from rocks are nearly indistinguishable from the modeled land mine.

ACKNOWLEDGMENT

The authors would like to thank the Signature Technology Lab, Georgia Tech Research Institute (GTRI), for use of their measurement facilities. They would also like to thank G. Wichmann of Heidelberg, Germany, for sharing some of the results of his research on empirically designed resistively loaded antennas and Dr. K. Steinbach, U.S. Army, European Research Office, for his support.

REFERENCES

[1] B. Boutros-Ghali, "The land mine crisis," *Foreign Affairs*, vol. 73, no. 5, pp. 8–13, Sept./Oct. 1994.
[2] *Hidden Killers 1994: The Global Landmine Crisis*. Washington, DC: U.S. Dept. State, Jan. 27, 1995.
[3] T. P. Montoya and G. S. Smith, "A study of pulse radiation from several broad-band loaded monopoles," *IEEE Trans. Antennas Propagat.*, vol. 44, pp. 1172–1182, Aug. 1996.
[4] ——, "Vee dipoles with resistive loading for short-pulse ground penetrating radar," *Microwave Optical Tech. Lett.*, vol. 13, no. 3, pp. 132–137, Oct. 1996.
[5] "Instruction sheet: Target, mine detection, EM inert," Rep. VSE Corp.., Alexandria, VA.

[6] *Former Yugoslavia Mine Data*, 1st Canadian Div. Eng. 613-541-5010 (ext. 4323), CSN 270-4323.
[7] *Engineer Contingency Handbook (Former Yugoslavia)*, Commandant, U.S. Army Eng. School, ATTN: ATSE-T-PD-P, Ft. Leonard Wood, MO, July 1993.
[8] J. E. Hipp, "Soil electromagnetic parameters as functions of frequency, soil density, and soil moisture," *Proc. IEEE*, vol. 62, pp. 98–103, Jan. 1974.
[9] R. W. P. King and G. S. Smith, *Antennas in Matter: Fundamentals, Theory, and Applications*. Cambridge, MA: MIT Press, 1981, ch. 6.
[10] G. S. Smith and W. R. Scott, Jr., "The use of emulsions to represent dielectric materials in electromagnetic scale models," *IEEE Trans. Antennas Propagat.*, vol. 38, pp. 323–334, Mar. 1990.
[11] W. R. Scott, Jr. and G. S. Smith, "Measured electrical parameters of soil as functions of frequency and moisture content," *IEEE Trans. Geosci. Remote Sensing*, vol. 30, pp. 621–623, May 1992.
[12] T. P. Montoya, "Vee dipole antennas for use in short-pulse ground-penetrating radars," Ph.D. dissertation, Georgia Inst. Technol., Atlanta, GA, Mar. 1998.
[13] K. S. Yee, "Numerical solution of initial boundary value problems involving Maxwell's equations in isotropic media," *IEEE Trans. Antennas Propagat.*, vol. AP-14, pp. 302–307, May 1966.
[14] K. L. Shlager and J. B. Schneider, "A selective survey of the finite-difference time-domain literature," *IEEE Antennas Propagat. Mag.*, vol. 37, pp. 39–57, Aug. 1995.
[15] K. S. Kunz and R. J. Luebbers, *The Finite Difference Time Domain Method for Electromagnetics*. Boca Raton, FL: CRC, 1993.
[16] A. Taflove, *Computational Electrodynamics, The Finite-Difference Time-Domain Method*. Norwood, MA: Artech House, 1995.
[17] J.-P. Bérenger, "A perfectly matched layer for the absorption of electromagnetic waves," *J. Computat. Phys.*, vol. 114, pp. 185–200, Oct. 1994.
[18] Z. S. Sacks, D. M. Kingsland, R. Lee, and J.-F. Lee, "A perfectly matched anisotropic absorber for use as an absorbing boundary condition," *IEEE Trans. Antennas Propagat.*, vol. 43, pp. 1460–1463, Dec. 1995.
[19] S. D. Gedney, "An anisotropic PML absorbing boundary media for the FDTD simulation of fields in lossy and dispersive media," *Electromagn.*, vol. 16, pp. 399–415, July/Aug. 1996.
[20] _____, "An anisotropic perfectly matched layer-absorbing medium for the truncation of FDTD lattices," *IEEE Trans. Antennas Propagat.*, vol. 44, pp. 1630–1639, Dec. 1996.
[21] D. C. Wittner and R. W. Ziolkowski, "How to design the imperfect Berenger PML," *Electromagn.*, vol. 16, no. 3, pp. 465–485, July/Aug. 1996.
[22] J. G. Maloney, K. L. Shlager, and G. S. Smith, "A simple FDTD model for transient excitation of antennas by transmission lines," *IEEE Trans. Antennas Propagat.*, vol. 42, pp. 289–292, Feb. 1994.
[23] S. O. Nelson, D. P. Lindroth, and R. L. Blake, "Dielectric properties of selected minerals at 1 to 22 GHz," *Geophys.*, vol. 54, no. 10, pp. 1344–1349, Oct. 1996.
[24] A. von Hippel, Editor, *Dielectric Materials and Applications*. Norwood, MA: Artech House, 1995, pp. 332–334.
[25] D. M. Pozar, *Microwave Engineering*. Reading, MA: Addison-Wesley, 1990, pp. 714–715.
[26] W. R. Humbert, "A new technique for measuring the electromagnetic properties of rotationally symmetric materials," Ph.D. dissertation, Georgia Inst. Technol., Atlanta, GA, June 1997.

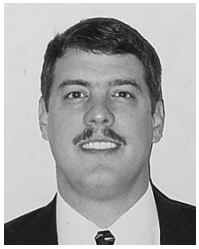

Thomas P. Montoya (S'85–M'87–S'92–M'98) received the B.S.E.E. and B.Phys. degrees from the South Dakota School of Mines and Technology, Rapid City, SD, in 1987, the M.S.E.E. from the University of Colorado, Colorado Springs, in 1992, and the Ph.D. degree from the Georgia Institute of Technology, Atlanta, in 1998.

In 1987, he served as a Commissioned Officer in the United States Army, and continued to serve in the United States Army Reserve from 1987 to 1997. From 1988 to 1991 he worked as an Electrical Design Engineer for the Defense Group of Texas Instruments, Colorado Springs. From 1991 to 1994 he was a National Defense Science and Engineering Graduate (NDSEG) and Georgia Tech Presidential Fellow and from 1991 to 1998 a Graduate Research and Teaching Assistant, Georgia Institute of Technology. In 1998 he joined the faculty of the department of Electrical Engineering at the University of Tennessee, Knoxville, TN, where he is currently an Assistant Professor. His technical interests include electromagnetics with a particular interest in antennas, short-pulse ground penetrating radars, and numerical modeling (e.g., the finite-difference time-domain method).

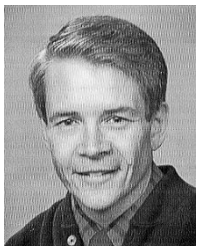

Glenn S. Smith (S'65–M'72–SM'80–F'86) received the B.S.E.E. degree from Tufts University, Medford, MA, in 1967, and the S.M. and Ph.D. degrees in applied physics from Harvard University, Cambridge, MA, in 1968 and 1972, respectively.

From 1972 to 1975, he served as a Postdoctoral Research Fellow at Harvard University and also as a part-time Research Associate and Instructor at Northeastern University, Boston, MA. In 1975 he joined the faculty of the School of Electrical and Computer Engineering at the Georgia Institute of Technology, Atlanta, where he is currently Regents' Professor and John Pippin Chair in electromagnetics. He is the author of *An Introduction to Classical Electromagnetic Radiation* (Cambridge, MA: Cambridge Univ. Press, 1997) and coauthor of *Antennas in Matter: Fundamentals, Theory, and Applications* (Cambridge, MA: MIT Press, 1981). He also authored the chapter, "Loop Antennas" in *Antenna Engineering Handbook* (New York: McGraw-Hill, 1993). His technical interests include basic electromagnetic theory and measurements, antennas and wave propagation in materials, and the radiation and reception of pulses by antennas.

Dr. Smith is a member of Tau Beta Pi, Eta Kappa Nu, and Sigma Xi, and the URSI Commissions A and B.